Intelligent Service Robotics (2024) 17:389–399
https://doi.org/10.1007/s11370-024-00516-7

ORIGINAL RESEARCH PAPER

Posture-dependent variable transmission mechanism for prosthetic hand inspired by human grasping characteristics

Mun Hyeok Chang[1] · Inchul Jung[1] · Kang Woo Seo[2] · Jonghoo Park[1] · Hyungmin Choi[1] · Kyu-Jin Cho[1]

Received: 5 November 2023 / Accepted: 12 January 2024 / Published online: 6 April 2024

Abstract
Gripping objects firmly and quickly is an important function of the human hand for everyday life. Prosthetic devices face significant challenges in replicating these capabilities, particularly in achieving a delicate balance between swift grasping and substantial grip strength while adhering to weight and form-factor constraints. To address these challenges, this study introduces a novel posture-dependent variable transmission (PDVT) that mimics the human hand's behavior by employing a spiral-shaped spool. The PDVT's spiral-shaped spool replicates the human hand's quick and gentle pre-contact movements followed by a stronger force application after contact with the object. Additionally, a compressive series elastic spring enhances tendon tension across a wide range of finger postures. The manufacturing method of PDVT, utilizing both 3D printing and metal processing, enables the creation of complex spiral shapes. The PDVT demonstrates improvements in both speed and grip strength compared to conventional rigid spool mechanisms. The PDVT has the potential to be applied to various robotic grasping systems.

Keywords Prosthetic hand · Variable transmission · Tendon-driven · Under-actuation

1 Introduction

Humans use various tools to interact with the external environment and perform tasks that can hardly be done with bare hands like hunting, carpentry, sports, and more [1, 2]. While performing such tasks, humans can grasp a tool firmly with their hands, ensuring the stability to manipulate it even under external forces and impact due to the interaction [3, 4]. Moreover, human hands can make firm grasps rapidly, which can be advantageous in changing grips for dexterous manipulation of a tool or in catching fast-moving objects that are free-falling or thrown [5]. In fact, the maximum grip strength of a human hand is approximately 400 N, while grip speed can reach up to 40 rad/s [6]. In the prosthetic industry, numerous prosthetic hands have been developed to replicate the grasping speed and force of the human hand. To properly assist the daily activities of hand amputees, a prosthetic hand is recommended to produce 65 N of grip strength and 4 rad/s of grasp speed [6, 7]. However, commercially available prosthetic hands have not been able to satisfy both the grip force and speed simultaneously [7]. Although implementing a high-power motor that can generate sufficient torque at high rotational speed can solve the issue, such high-power motors often exceed the size and weight limitation of prosthetic hands. As being lightweight and compact is one of the most important features, most prosthetic hands are equipped with small motors that offer limited grasping capabilities compared to a human hand.

To address the issue of insufficient motor power, variable transmission mechanisms have been developed for prosthetic

✉ Kyu-Jin Cho
kjcho@snu.ac.kr

Mun Hyeok Chang
munhyuk89@snu.ac.kr

Inchul Jung
dlscjf410@snu.ac.kr

Kang Woo Seo
Kennyrain0302@gmail.com

Jonghoo Park
jpark608@snu.ac.kr

Hyungmin Choi
tndhals@snu.ac.kr

[1] School of Mechanical Engineering, Seoul National University, Gwanak-ro 1, Gwanak-gu, Seoul 08826, Republic of Korea

[2] School of Mechanical Engineering, Georgia Institute of Technology, North Avenue, Atlanta, GA 30332, USA

hands, primarily using tendon-driven systems. The mechanisms are designed to adjust the ratio of motor speed and force, selectively achieving rapid speed and strong force in grasping. A prominent example of the variable transmission mechanism is the twisted string actuation (TSA) mechanism [8–11] which generates linear motion from twisting the string, or tendon. By changing the mode of twisting through additional actuation, it is possible to adjust the grasping speed and force, which have an inverse-proportional relationship. This enables the prosthetic fingers to be operated either at high speed or with substantial force. Another example of the variable transmission mechanisms using tendons is the ones with variable spool or pulley diameters [12–14]. Spools or pulleys with varying diameters due to external forces, along with a single motor, allow for rapid joint movement in the absence of external forces and increase joint torque when external forces are applied. To change the diameter of the spool due to external forces, elastic materials were used to make the spool, and it can be used up to 49 times in high-force mode [12]. Other variable transmission mechanisms like planetary gears, moment arm modification, or gear-based locking variable transmission mechanisms have been developed [15–19].

In this study, a posture-dependent variable transmission (PDVT) was developed to achieve high speed and force in grasping, inspired by the characteristics of human grasping. Human muscles exhibit faster speeds when lower force is required and slower speeds when greater force is needed [20]. Similarly, the human hand can move rapidly before making contact with an object, requiring less muscle force, and increases its force after contact. To mimic these hand characteristics, a spiral spool was designed with a continuously decreasing diameter for the tendon to wind around (Fig. 1). When the contact posture between the object and the finger is predetermined, the spiral spool winds the tendon around the relatively large diameter of the spool before contact to allow the finger to move rapidly. After contact, the tendon is wound around the relatively small diameter of the spool to enable a strong grip on the object. Additionally, the compression spring connected in series to the tendon allows it to continue winding around the smaller diameter of the spiral spool even after contact with the object, increasing tendon tension. As a result, the developed PDVT can generate rapid finger movements and exert high grasping forces in specific contact postures. The manufacturing method of PDVT, which combines 3D printing and metal processing, allows for the creation of complex spiral shapes. In this study, we explore the characteristics of PDVT through a parameter study of the spiral spool and spring, determining suitable features for applying PDVT to prosthetic fingers. We design PDVT for two contact cases using the characteristics identified through parameter studies of springs and spiral spools and validate their performance through experiments. When using the same motor, fingers equipped with the PDVT mechanisms are up to 3.7 times faster in grasping speed and up to 5 times stronger in grip force compared to fingers with a constant diameter rigid spool.

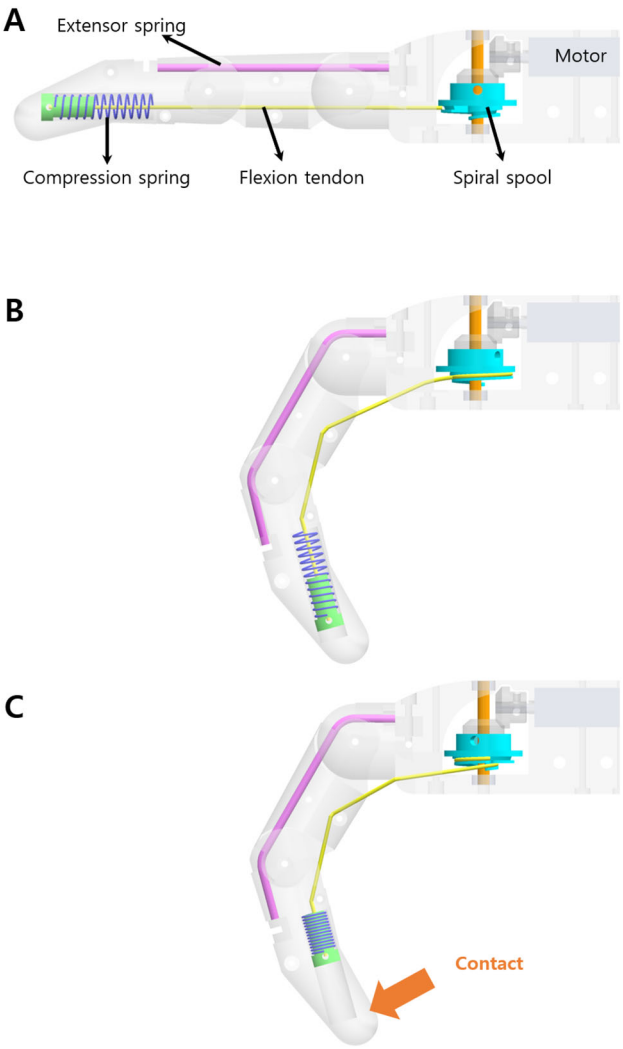

Fig. 1 Posture-Dependent Variable Transmission(PDVT). **a** PDVT design. **b** A PDVT operation before making contact with an object. **c** A PDVT operation after making contact with an object

2 PDVT design

2.1 Principle of PDVT

PDVT is a variable transmission mechanism that varies finger flexion speed and the maximum tension in the flexion tendon according to finger posture. PDVT consists of a spiral spool and a series elastic compression spring (Fig. 1a). PDVT changes finger flexion speed and flexion tendon tension through two processes.

Process 1: Before the finger makes contact with the object, PDVT bends the finger by winding the flexion tendon around

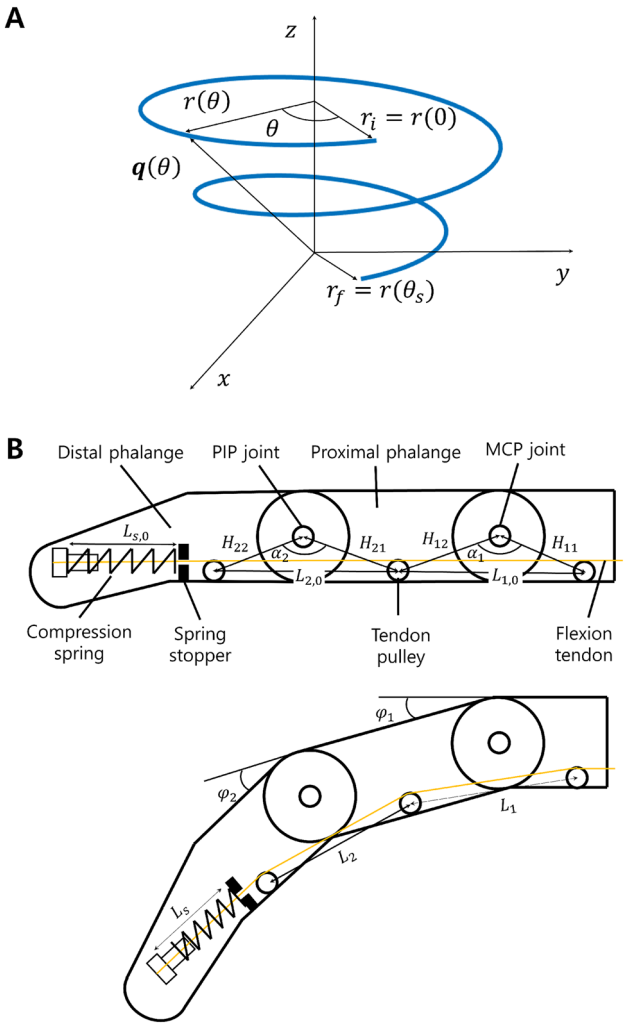

Fig. 2 Schematics of a PDVT finger. **a** Schematics of a spiral spool. **b** Schematics of a PDVT finger with compression spring

the spiral spool (Fig. 1b). Spiral spool rotates with the tendon winding in a spiral shape, and the radius of the spool decreases gradually as it winds. The required tension to bend the finger in the flexion tendon compresses the spring. The amount of tendon winding around the spool until the finger makes contact with the object is the sum of the change in tendon length required to move the finger and the compression length of the series elastic compression spring.

Process 2: After the finger comes into contact with the object, the compression spring compresses further, and the flexion tendon winds more around the spiral spool. As the winding length of the tendon increases, the radius of the spiral spool decreases, allowing it to transmit higher tension to the flexion tendon at the same torque. When the compression spring is fully compressed, the motor increases the torque up to the stall torque. At this point, the tension is the maximum tension applied by the sprial spool to the tendon.

2.2 PDVT modeling

We designed the maximum tension in the tendon and grasping speed based on the posture of the fingers by adjusting the design parameters of the spiral spool and the series elastic compression spring. The maximum tension of the tendon depending on the finger's posture was obtained by calculating the relationship between the finger's flexion angle and the length of tendon wound on the spool and the spool's radius corresponding to the length of tendon wound on the spool. Grasping speed can be obtained by calculating the motor's rotation angle required to create the finger's posture.

The radius of the spiral spool based on the length of the wound tendon (i.e., rotational angle of spool) is designed by varying the radius ratio of the spiral curve and the length of the spiral curve. The radius ratio (r_{ratio}) of the spiral spool is defined as the ratio between the initial radius and the final radius, as shown in Eq. (1).

$$r_{\text{ratio}} = \frac{r_i}{r_f} \tag{1}$$

r_i represents the initial radius of the spiral curve, and r_f represents the final radius of the spiral curve (Fig. 2a). The PDVT's spiral spool is designed to have the tendon winding onto the spool having a constant radius (i.e., r_f) with the final radius after the tendon has wound in the spiral curve shape.

The length of the spiral curve(L_{spiral}) is given by Eq. (2).

$$L_{\text{spiral}} = \int_0^{\theta_s} \left| \frac{\mathrm{d}q(\theta)}{\mathrm{d}\theta} \right| \mathrm{d}\theta \tag{2}$$

θ represents the motor's spool rotation angle, and θ_s signifies the angle forming the spiral curve (Fig. 2a). q represents the position vector of the spiral curve, given by Eq. (3).

$$q(\theta) = r(\theta)\cos(\theta)\hat{i} + r(\theta)\sin(\theta)\hat{j} + p\theta\hat{k} \tag{3}$$

$r(\theta)$ represents the varying radius value with respect to θ, and p is the pitch of the spiral curve. $r(\theta)$ is calculated as shown in Eq. (4).

$$r(\theta) = r_i + \frac{r_f - r_i}{\theta_s}(\theta) \tag{4}$$

The length of the tendon wound around the PDVT's spool to create a finger posture (ΔL) was calculated from Eqs. (1)–(4), as shown in Eq. (5).

$$\Delta L = \begin{cases} \int_0^{\theta_m} \left| \frac{\mathrm{d}q(\theta)}{\mathrm{d}\theta} \right| \mathrm{d}\theta & (\theta_{\text{m}} \le \theta_s) \\ \int_0^{\theta_s} \left| \frac{\mathrm{d}q(\theta)}{\mathrm{d}\theta} \right| \mathrm{d}\theta + r(\theta_s)(\theta_m - \theta_s) & (\theta_m > \theta_s) \end{cases} \tag{5}$$

Fig. 3 Under-actuated PDVT finger free movement

θ_m represents the magnitude of the final angle that the PDVT spool rotates to create a finger posture. θ_m was calculated from Eq. (5). Once θ_m is determined, the maximum tension ($T_{\max}$) in the flexion tendon was calculated using Eq. (6).

$$T_{\max} = \frac{\tau_{\max}}{r(\theta_m)} \tag{6}$$

The $\tau_{\max}$ represents the motor's stall torque. To increase tension at the same stall torque, $r(\theta_m)$ should decrease. By using Eqs. (5) and (6), we can determine the maximum tension of the tendon based on the length of the tendon wound around the spool. Calculating the length of the tendon wound around the spool based on the finger's posture allows us to calculate the maximum tension of the tendon for that specific finger posture, in conjunction with Eqs. (5) and (6).

During the bending of the finger, the length of the tendon wound around the spool (ΔL) is given by the sum of the changes in the distance between the tendon pulleys and the length of the spring, as shown in Eq. (7) (Fig. 2b).

$$\Delta L = L_{1,0} - L_1 + L_{2,0} - L_2 + L_{s,0} - L_s \tag{7}$$

The finger equipped with PDVT features a tendon-driven under-actuation mechanism to enable adaptable grasping of object shapes (Fig. 2b) [21]. In order to grasp objects of various sizes, the positions of the tendon pulleys in the finger with tendon-driven under-actuation are designed to allow flexion of the PIP joint after the MCP joint has flexed ($H_{11} = 15.3\,\text{mm}$, $H_{12} = 20.0\,\text{mm}$, $H_{21} = 18.1\,\text{mm}$, $H_{22} = 12.6\,\text{mm}$, $\alpha_1 = 2.36\,\text{rad}$, $\alpha_2 = 2.27\,\text{rad}$). A finger equipped with PDVT first moves the proximal phalanx. After the proximal phalanx has moved into contact with the object or within its range of motion, the distal phalanx then moves. The free movement of the designed finger is illustrated in Fig. 3.

The distance between the tendon pulleys ($L_{1,0}$, $L_{2,0}$) before the finger bends is given by Eq. (8).

$$L_{i,0} = \sqrt{H_{i,1}^2 + H_{i,2}^2 - 2H_{i,1}H_{i,2}\cos(\alpha_i)} \quad (i = 1, 2) \tag{8}$$

The distance between the tendon pulleys (L_1, L_2) after the finger bends is given by Eq. (9).

$$L_i = \sqrt{H_{i,1}^2 + H_{i,2}^2 - 2H_{i,1}H_{i,2}\cos(\alpha_i - \phi_i)} \quad (i = 1, 2) \tag{9}$$

The MCP joint flexion angle is ϕ_1, and the PIP joint flexion angle is ϕ_2. The sum of the flexion angles of the two joints (ϕ_f) is given by Eq. (10).

$$\phi_f = \phi_1 + \phi_2 \tag{10}$$

The length change of the compressive spring connected in series to the tendon during finger flexion is determined by the tension of the tendon required to flex the finger. The function of tension with respect to the flexion angle of the finger is denoted as $T(\phi_f)$, and when the spring constant of the compressive spring is represented as K, the length change of the spring is given by Eq. (11).

$$L_{s,0} - L_s = \frac{T(\phi_f)}{K} \tag{11}$$

The relationship between finger flexion angle and tendon tension, as determined through experiments, is detailed in Sect. 3.3's spring parametric study.

The changes in tendon length with respect to finger flexion angle before object contact are calculated using Eqs. (8), (9), and (11), by substituting them into Eq. (7). By utilizing the calculated changes in tendon length with respect to finger flexion angle, motor rotation angles required to achieve finger flexion angles can be determined using Eq. (5). This establishes the relationship between the flexion angle of the finger with PDVT applied and the motor rotation angle. When the finger makes contact with an object and the tension in the tendon reaches its maximum, the compression length of the spring (i.e., $L_{s,0} - L_s$) becomes equal to the spring's allowable compression length. By applying the spring's allowable compression length to Eqs. (7) and 5, the motor rotation angle corresponding to the maximum tension on the tendon can be calculated. Utilizing this value in Eqs. (4) and (6) allows us to determine the maximum tension applied to the tendon in the finger's posture after object contact.

2.3 PDVT and finger fabrication

To create a novel spool with both a spiral shape and high durability, we employed a combination of 3D printing and

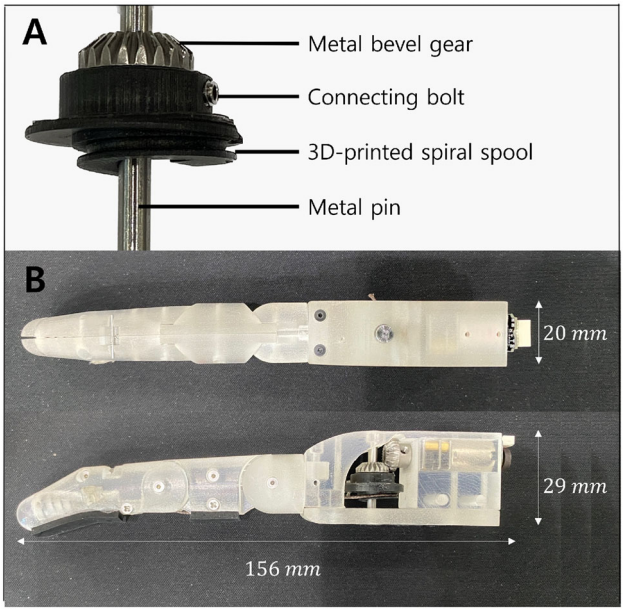

Fig. 4 PDVT finger fabrication. **a** Spiral spool fabrication. **b** PDVT finger fabrication

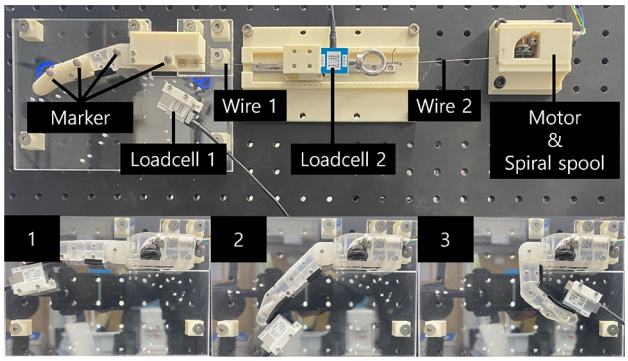

Fig. 5 Experimental setup

Table 1 Spiral spool geometries

	r_{ratio}	L_{spiral} (mm)
Spool I	5	30
Spool II	5	20
Spool III	2	30

metal machining. The portion of the spool with the spiral shape was manufactured using SLA (Stereolithography) type 3D printing (Figure 4 Jewelry, 3D Systems), which allowed us to create the intricate spiral pattern (Fig. 4a). The section responsible for maximizing wire tension was fabricated using steel material for increased strength, and metal pins were utilized in this area. The integration of the 3D printing component and the metal pins was achieved through the use of metal bolts, ensuring a secure and robust connection between the two parts.

The fingers equipped with PDVT were designed to fit within the 50th percentile size range of adult male hands (Fig. 4b) [22]. The finger incorporating PDVT were manufactured using a polyjet-based 3D printing process (J35 pro, Stratasys). The combination of 3D printing and metal processing in the PDVT-equipped fingers, including the motor, results in a weight of 70 g.

3 Parametric study

To better understand the characteristics of the modeled PDVT's spiral spool and compression spring in Sect. 2, we conducted a parametric study on the geometry of the spiral spool and the spring stiffness and lengths.

3.1 Parametric study test setup

An experimental setup for the parametric study of the PDVT was designed (Fig. 5). To measure the motor's rotating angle for finger posture, markers capable of measuring positions at each finger joint were attached, and motors equipped with encoders (Pololu 6V High-power micro geared motor 380:1, 1.1W) were used. The markers were tracked using a camera system (OptiTrack, NaturalPoint, Inc.). To measure contact between the fingers and objects at each position, loadcell 1 (Ktoyo, 5 kgf loadcell) was placed at stopping points to measure contact with objects. To measure the maximum tension of the tendon for finger posture, loadcell 2 (Ktoyo, 20 kgf loadcell) was connected between the finger's flexion tendon (wire 1) and the spiral spool's tendon (wire 2). Maximum fingertip force and maximum tendon tension were measured using the same method as in a previous study, which employed motors with the same power, involving the motor's stall torque value [12]. Measurements of the finger's flexion angle, maximum tension, and the motor's rotating angle were taken at three positions, as shown in Fig. 5.

3.2 Spiral spool parametric study

We conducted experiments with three different spool geometries, which are controlled by two parameters: the radius ratio of the spool and the length of the spiral curve on the spool (Table 1). We compared the finger's flexion speed and the maximum tendon tension with respect to changes in the length of the spiral curve using Spool 1 and Spool 2 (Fig. 6). We also examined the influence of differences in the radius ratio on the finger's flexion speed and maximum tendon tension using Spool 1 and Spool 3 (Fig. 6). When changing the radius ratio, we kept the maximum diameter fixed at 17.5 mm and varied the minimum diameter as a variable. The finger's

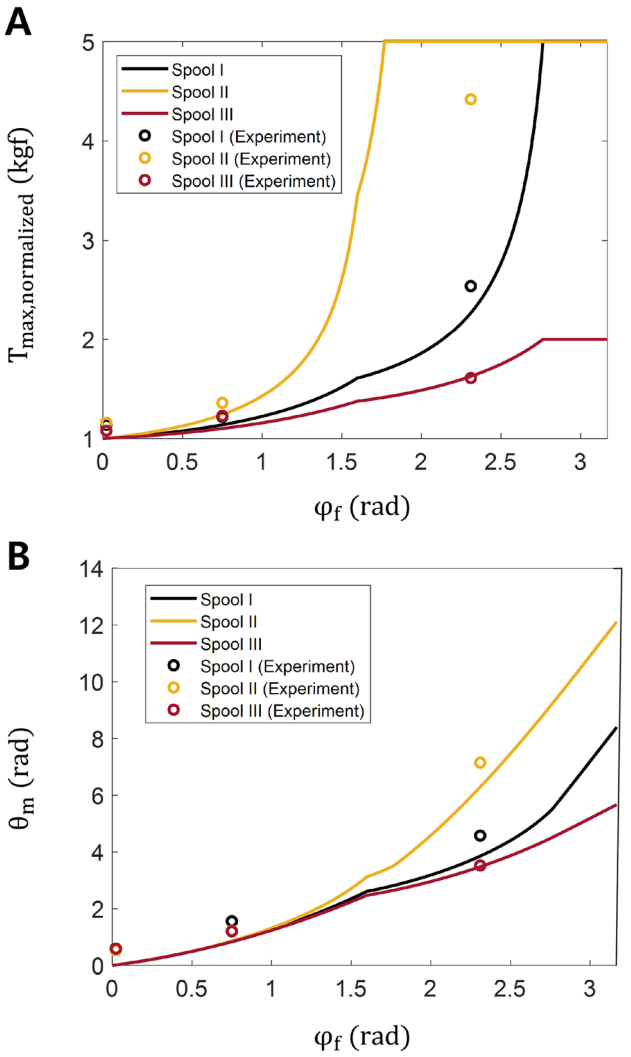

Fig. 6 Parameter experiments for spool geometry. **a** Normalized maximum tension versus finger flexion angle. **b** Motor rotation angle versus finger flexion angle

flexion speed was determined by measuring and modeling the motor angle required to achieve a specific finger flexion angle for each spool. A larger motor angle to achieve the same flexion angle indicates slower finger speed. We measured and modeled the maximum tendon tension based on the finger's flexion angle for each spool. A higher maximum tendon tension at the same finger flexion angle indicates that the finger exerts more force when gripping objects. The maximum tendon tension that a spool can produce is normalized in Eq. (12) based on the case where the spool's diameter is largest ($r = r_i$).

$$T_{\max,\text{normalized}} = \frac{T_{\max}(r = r(\theta_m))}{T_{\max}(r = r_i)} \tag{12}$$

The PDVT spiral spool's angle of rotation required for the spool and the normalized maximum tension change with the length of the spiral portion to achieve the same tendon length pull (Fig. 6). As the length of the spiral curve on the spool decreases, the range where the normalized maximum tension is at its peak becomes longer (Fig. 6a). A shorter length of the spiral curve allows the wire to wind onto the minimum diameter spool more quickly, enabling the spool to deliver maximum tension over a broader range of finger postures. However, as the length of the spiral curve decreases, the finger's speed decreases (Fig. 6b). A shorter spiral curve increases the length of wire wound onto the minimum diameter spool, requiring the spool to rotate through a larger angle. A larger rotation angle means that more time is required to pull the same tendon length, resulting in slower finger movement. Conversely, a longer spiral portion allows the spool to deliver maximum tension to the tendon over a narrower range of finger postures, increasing finger speed. When designing PDVT, this trade-off should be considered.

Table 2 Spring characteristics

	K (N/mm)	L_{spring} (mm)
Spring I	0.755	15
Spring II	0.755	3
Spring III	0.098	18.5

The PDVT spiral spool's angle of rotation required for the spool and the normalized maximum tension change with the diameter ratio to achieve the same tendon length pull (Fig. 6). As the diameter ratio increases, the minimum diameter decreases, leading to an increase in normalized maximum tension (Fig. 6a). A higher normalized maximum tension means that the finger can exert stronger force in the same finger posture, and to increase finger strength, it is necessary to design a larger diameter ratio. However, increasing the diameter ratio in the spiral spool slows down the finger's speed (Fig. 6b). A larger diameter ratio results in a larger angle of rotation required for the spool to create the same spiral curve length. An increased angle of rotation needed for the spool to achieve the same posture means that the finger's speed decreases. When comparing Spool I and Spool III, it's evident that the larger diameter ratio in Spool I results in a normalized maximum tension difference of up to 2.5 times, but the speed difference is a maximum of 1.5 times. Spool I with a larger diameter ratio is a more efficient choice for the PDVT finger. We applied this diameter ratio to the spiral spool in our design.

3.3 Spring parametric study

The design parameters for the spring are the maximum compression length of the spring and the spring stiffness. We conducted experiments with three types of springs as shown in Table 2 to understand their impact. In Table 2, L_{spring} rep-

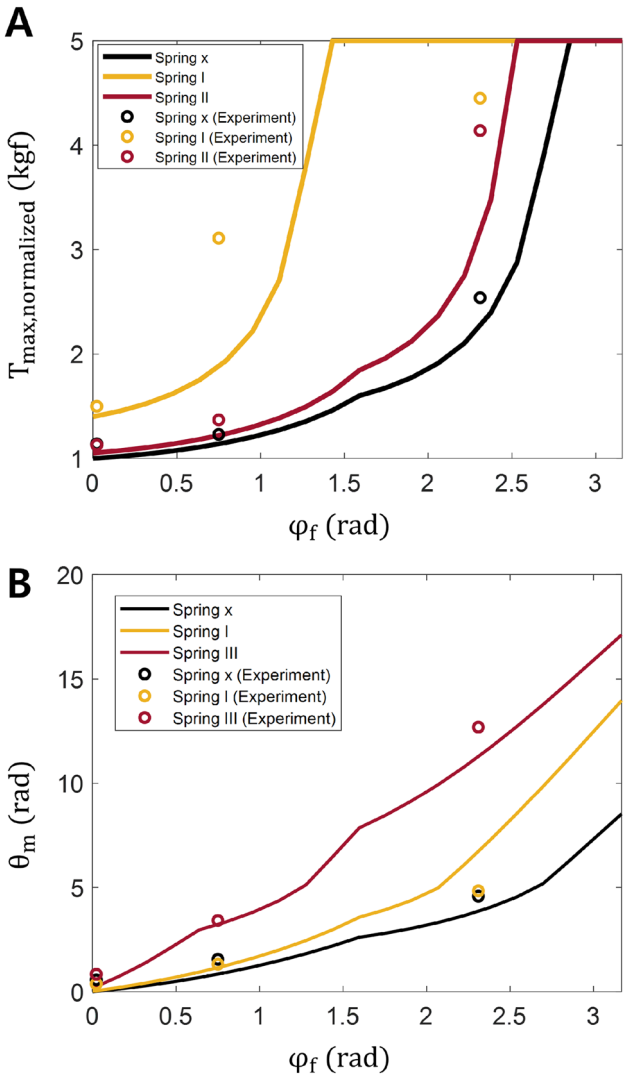

Fig. 7 Parameter experiments for spring characteristics. **a** Normalized maximum tension versus finger flexion angle. **b** Motor rotation angle versus finger flexion angle

resents the allowable compression length of the spring. To isolate the effect of the spring, we kept the diameter ratio of the spiral spool and the length of the spiral curve constant. Comparisons were made using Spring I and Spring II to analyze the change in the maximum tension of the tendon with varying maximum compression length of the spring (Fig. 7a). By comparing Spring I and Spring III, we assessed how the difference in spring stiffness affects the finger's flexion speed (Fig. 7b). The finger's flexion speed was measured by determining the motor angle required to create the finger's flexion angle and modeling it for each spool. A larger motor angle required to achieve the same flexion angle indicates slower finger speed. We also measured and modeled the maximum tendon tension based on the finger's flexion angle. A higher tendon tension at the same finger flexion angle indicates that the finger can exert a stronger force when gripping objects.

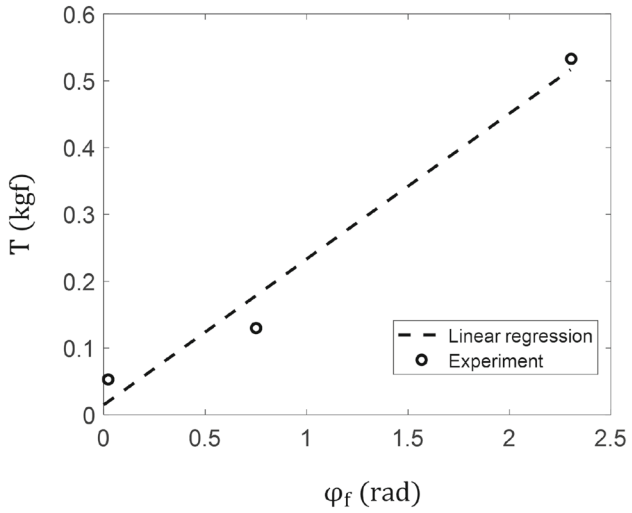

Fig. 8 Tendon tension during finger flexion

After the finger makes contact with an object, the PDVT's spiral spool winds more tendon onto itself as the spring compresses. Adding tendon equal to the amount of spring compression ensures that, in the same finger posture, the tendon is wound onto a smaller-diameter spool, resulting in a higher tension transmitted to the tendon. As the amount of spring compression increases, the PDVT enhances the tension delivered by the spool to the tendon in the same finger posture (Fig. 7a). To maximize spring compression, the spring must have a long allowable displacement.

When the stiffness of the spring changes, the PDVT adjusts the required rotation angle of the spool to achieve the finger's posture. The spring is pulled during finger movement to match the tension required to fold the finger. To model the length of the spring that compresses during finger flexion, we measured the tension in the tendon required to fold the finger at different flexion angles and approximated it with a first-order equation (Fig. 8, Eq. (13)).

$$T(\phi_f) = 0.2181 * \phi_f + 0.0150 \tag{13}$$

By substituting the relationship between tendon tension and finger flexion angle from Eq. (13) and the spring stiffness K from Table 2 into Eq. (11), the compression length of the spring for the finger's flexion angle was calculated. By substituting the calculated compression length of the spring into Eqs. (7) and (5), the relationship between the finger flexion angle and the motor's rotation angle was established (Fig. 7b).

A lower spring stiffness results in a longer length being pulled during finger movement, which leads to an increase in the motor's rotation angle required to achieve the same flexion angle (Fig. 7b). An increase in motor rotation angle

indicates an increase in the time needed to achieve the same flexion angle, resulting in slower finger movement.

From the two parametric studies, it can be observed that higher spring stiffness leads to faster finger movement, and a larger allowable displacement of the spring increases tendon tension. However, prosthetic fingers with sizes similar to human fingers have limitations in terms of applicable spring length and size. Therefore, we applied spring 1, which had both high stiffness and compression length values, from the parametric study to the PDVT.

As discussed in Sect. 3.2, there is a trade-off in the design of the spiral spool, where increasing the length of the spiral curve results in faster finger speed but reduces the range of finger postures with the maximum tension achievable by PDVT. The PDVT, with springs connected in series to the tendon, addresses this trade-off by extending the range of finger postures with the maximum tension achievable by PDVT, thereby overcoming the trade-off between speed and force. Designing a longer spiral curve and matching the compression length of the spring to the length of the spiral curve allows the PDVT-applied finger to grasp objects quickly and exert maximum tension on the flexion tendon in all finger postures. However, due to the limitations of the spring length that can be applied to the fingers, spring 1, which we used for PDVT, cannot apply maximum tension to the flexion tendon in all finger postures for spiral spools with a spiral curve length exceeding 15 mm. Therefore, to apply the proposed PDVT to prosthetic fingers, it should be considered based on finger postures where maximum tension can be applied to the tendon.

4 PDVT finger performance

Based on the results of the parametric study in Sect. 3, we designed and applied PDVT to the fingers for two use cases. The first use case involves applying the maximum tension that PDVT can generate to the tendon in all finger postures after the fingers have made contact with an object in order to securely grasp objects of various sizes. In this case, since the tendon must be wound around the PDVT spool at its minimum diameter in all postures, the size of the allowable compression length of the spring and the spiral length of the spiral spool should be the same. In Sect. 3, the allowable compression length of the spring chosen for application to the fingers was 15 mm, so the spiral length of the spiral spool for the first case is 15 mm. We will refer to this PDVT with the applied spool as PDVT I.

The second use case involves grasping objects with a small diameter quickly and firmly, such as gripping a tennis racket. In the second case, the design is aimed at delivering the maximum tension that PDVT can generate to the tendon when the finger grips a cylinder with a diameter of 35 mm or less. We chose the 35 mm diameter cylinder as a reference because it is similar to the handle diameter of tools where human grip strength is maximized [23]. In this case, the length of the spiral is determined by the change in tendon length in the finger to create the finger flexion angle required to grip a 35 mm diameter cylinder, plus the allowable compression length of the spring. We applied PDVT to the fingers to grip a 35 mm diameter cylinder and measured the finger flexion angle. The finger posture at the measured finger flexion angle corresponds to Position 3 in the experimental setup of Fig. 7. The change in tendon length in the finger required to achieve this flexion angle is 26.8 mm, and the spiral length of the spool, including the allowable compression length of the spring, is 41.8 mm. We will refer to this PDVT with the applied spool as PDVT II.

To evaluate the performance of fingers with PDVT applied, grip force and grasping speed experiments were conducted for four different transmissions: large spool (spool I, $r = 17.5$ mm), small spool (spool II, $r = 1.75$ mm), PDVT I, and PDVT II. The grip force experiments were conducted for three different finger postures (Fig. 9a–c). Grasping speed was measured as the time it took for the fingertip to reach position 3 (Fig. 9d).

In the grip force experiments, the fingers with PDVT applied exhibited higher fingertip forces compared to the fingers with a large spool in all positions. The reason for the higher fingertip force in Position 1 for the fingers with PDVT applied compared to those with a large spool is that PDVT causes the tendon to wind around a smaller diameter of the spiral spool due to the spring's compression. In all finger postures, PDVT I was designed to generate the same force as the small spool. It can be observed that the fingers with PDVT I applied produce higher fingertip forces compared to the fingers with a small spool in all finger postures. In the case of the small spool, there is an effect where the wires overlap and temporarily increase the diameter, which appears to result in the fingers with PDVT I applied generating greater fingertip forces. Fingers with PDVT I applied can produce forces ranging from 1.5 to 2.4 kgf, depending on the posture.

PDVT 2 was designed to produce the same force as the small spool starting from Position 3. In Positions 1 and 2, PDVT II generates less force than the small spool, but in Position 3, it produces even greater force than the small spool. The reason why the fingers with PDVT II applied generate more force than PDVT 1 and the small spool in Position 3 is because there is no phenomenon of wires overlapping and increasing the diameter. Fingers with PDVT II applied can produce forces ranging from 0.52 to 2.5 kgf, depending on the posture.

The speed experiment results show that both fingers with PDVT applied take less time to grasp compared to the fingers with the small spool. The grasping time for the finger with

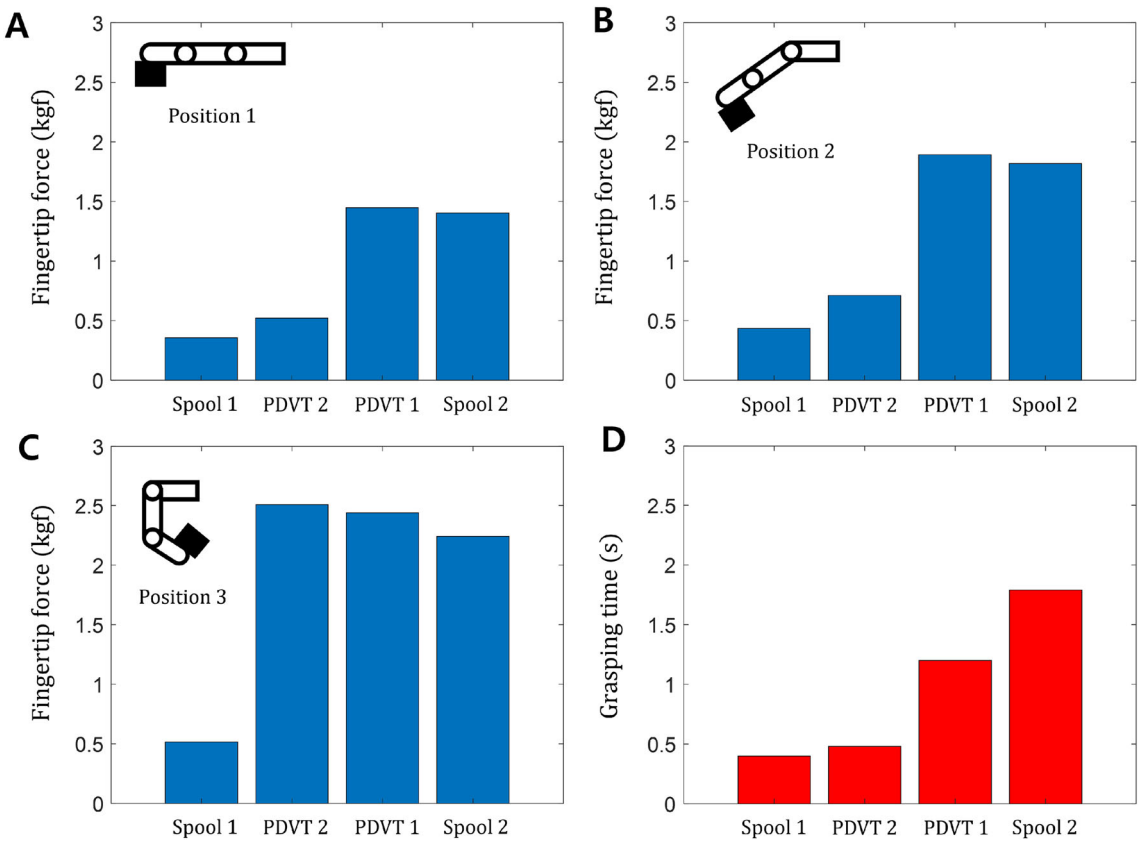

Fig. 9 PDVT finger performance. **a** Fingertip force of the fingers with each spool in position 1. **b** Fingertip force of the fingers with each spool in position 2. **c** Fingertip force of the fingers with each spool in position 3. **d** Grasping time required to achieve the posture of position 3 in the experimental setup (Fig. 4)

PDVT I applied is 1.2 s, which is 1.5 times shorter than the grasping time for the finger with the small spool applied. The grasping time for the finger with PDVT II applied is 0.48 s, which is 3.7 times shorter than the grasping time for the finger with the small spool applied.

To assess the durability of PDVT, repetitive cycling experiments were conducted. The durability test involves repeatedly measuring the motor angle using a motor encoder when the fingertip force reaches 2.5 kgf. According to the results of the repetitive cycling experiments, there were no issues with the spiral spool after a total of 311 repetitions for PDVT I and 409 repetitions for PDVT II; however, the tendon eventually broke. It was possible to maintain the same fingertip force at the same encoder angle until the tendon broke. (Fig. 10).

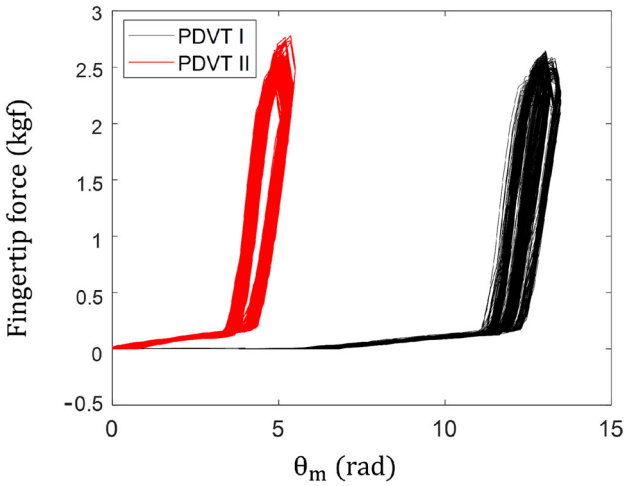

Fig. 10 PDVT finger durability test

5 Conclusion

In this study, we have developed a variable transmission mechanism that mimics how humans adjust their grasping speed and force when gripping objects. The PDVT consists of a spiral-shaped spool with a decreasing diameter where the tendon winds, and it is connected in series to a compression spring. The PDVT operates by winding the tendon around a relatively large-diameter spool before contact between the object and the finger, allowing for rapid movement. After contact, the tendon is wound around a smaller

Table 3 Performances of developed variable transmission mechanisms

Variable transmission	Number of actuators	Grasping time (s)	Fingertip force (N)	Cycle
Jeong [9]	2	0.8	48.2	28,500/3005
Takaki [15]	2	0.47	22	–/–
O'Brien [12]	1	0.45	32	2497/49
PDVT I	1	0.48	25	–/311
PDVT II	1	1.2	25	–/409

diameter, delivering a strong force to the object. The compression spring extends the tendon winding length around the spiral spool after finger contact with an object, increasing tendon tension.

We conducted a parametric study to understand the characteristics of PDVT by investigating the design parameters of the spiral spool and compression spring. Through the parametric study, we confirmed that a higher diameter ratio of the spiral spool allows for more efficient utilization of motor power. Additionally, we found that the design of the spiral curve length enables the adjustment of the tension applied to the tendon and the finger's speed. In the case of the compression spring, our parametric study revealed that a higher spring stiffness results in faster finger movement. A longer compression length of the spring allows the spool to exert maximum tension on the tendon over a wider range. If the spring is long enough, it is possible to design the spiral length sufficiently long, allowing for fast speed and strong fingertip force in all finger postures. However, since prosthetic fingers need to be similar in size to human fingers, there are limitations on the size and length of the available spring. This limitation was confirmed through parametric study, which revealed that there is a trade-off between force and speed depending on the spiral length. The modeling and experimental results in the parametric study showed a similar trend. The differences between experimental results and modeling arise from our assumption during modeling that the wire was inextensible. In the experiments, the wire stretched, leading to variations in the length it winds around the spool and occasionally causing overlapping.

We designed and experimentally verified the performance of PDVT by applying the design features determined from the parameter study to the fingers. PDVT was designed for two cases: one with slow but strong force in all postures and the other with fast but strong force in specific postures. The case with slow but strong force in all postures maintains a constant diameter in all finger postures, resulting in similar force compared to a spool with the minimum diameter of the spiral spool. However, it achieves a grasping speed that is 1.5 times faster. On the other hand, the case with fast but strong force in specific postures matches the minimum diameter of the spiral spool in the finger posture where humans exert the strongest force on a cylinder, resulting in similar force while achieving a grasping speed that is 3.7 times faster. The parametric study of PDVT and PDVT design based on specific use cases can serve as a design guideline for those wishing to apply PDVT to prosthetic hands.

The method of producing PDVT using 3D printing and metal pins simultaneously allows for the creation of a simplified and robust structure for the spiral spool, replacing its complex shape. In durability tests of the finger equipped with PDVT, which involved repeatedly exerting strong tension equivalent to 2.5 kgf, the structure of the spiral spool remained intact, and while the wire eventually broke, there was no evidence of structural degradation. The proposed PDVT is more robust compared to existing variable transmission spools that use soft materials [14], and it is anticipated that further enhancing wire durability can improve the overall durability of PDVT. By selectively using metal materials in necessary parts, the PDVT-equipped fingers weigh only 70 g when combined, making them lighter than conventional prosthetic hands [7].

We have compared our research with existing studies on tendon-driven variable transmission mechanisms through a table (Table 3). The fingertip forces in Table 3 represent the maximum fingertip force for each finger. Our proposed PDVT is simpler than variable transmission mechanisms that use two motors, as it utilizes a single motor [9, 15]. However, our study's performance in terms of force and speed is inferior to the study that use a spool with a changing diameter driven by external forces, as we use a spool with a gradually decreasing diameter [12]. Nevertheless, spools with a diameter that changes due to external forces can withstand over 49 uses in high-force mode due to spool shape deformation. According to previous research, for prosthetic fingers intended for everyday use, a grasping time of 1–1.5 s and a grip strength of 45 N are sufficient [24, 25]. Our proposed PDVTs satisfy the necessary fingertip force and grasping time for daily life while also being capable of operating for more than 300 cycles in high-force mode.

We believe that our proposed 3D printed prosthetic finger with PDVT can significantly enhance the quality of life for upper limb amputees. The proposed PDVT is versatile in design, making it applicable to various use cases in pros-

thetic hands. A PDVT capable of exerting strong force slowly across all postures can be applied to prosthetics for daily activities. On the other hand, a PDVT with rapid response and the ability to exert strong force in specific postures is suitable for tasks like sports or gripping tools such as hammers. This versatility is anticipated to enhance the social participation of amputees, ultimately improving their quality of life. Furthermore, in applications such as grippers where there is no limitation on spring length, our developed PDVT can be applied to tendon-driven gripper fingers, ensuring the delivery of maximum tension in all finger postures with rapid grasping speed. We believe that the proposed PDVT can be adaptable to various tendon-driven grasping mechanisms. In future, we plan to utilize fingers equipped with the PDVT to develop an anthropomorphic prosthetic hand. When developing the prosthesis, we will conduct design optimization of the PDVT based on the parametric study conducted in this research, tailored to the specific task. We will further enhance the developed prosthetic hand by incorporating additional features such as tactile sensors, enabling it to grasp and manipulate objects with various forces and providing advanced control capabilities.

Funding Open Access funding enabled and organized by Seoul National University. This work was supported by the Korea Medical Device Development Fund grant funded by the Korea government (the Ministry of Science and ICT, the Ministry of Trade, Industry and Energy, the Ministry of Health & Welfare, the Ministry of Food and Drug Safety) (Project Number: RS-2020-KD000175.

Declarations

Conflict of interest The authors declare no conflict of interest.

References

1. Peeters R, Simone L, Nelissen K et al (2009) The representation of tool use in humans and monkeys: common nd uniquely human features. J Neurosci 29(37):11523–11539
2. Young RW (2003) Evolution of the human hand: the role of throwing and clubbing. J Anat 202(1):165–174
3. Radwin RG, Armstrong TJ, Chaffin DB (1987) Power hand tool vibration effects on grip exertions. Ergonomics 30:833–855
4. Komi ER, Roberts JR, Rothberg SJ (2008) Measurement and analysis of grip force during a golf shot. Proc Inst Mech Eng Part P J Sports Eng Technol 222(1):23–35
5. Namiki A, Imai Y, Ishikawa M, Kaneko M (2003) Development of a high-speed multifingered hand system and its application to catching. In: International conference on intelligent robots and systems (IROS), pp 2666–2671
6. Weir RF (2003) Design of artificial arms and hands for prosthetic applications. In: Kutz M (ed) Standard handbook of biomedical engineering and design. McGraw-Hill, New York
7. Belter JT, Segil JL, Dollar AM, Weir RF (2013) Mechanical design and performance specifications of anthropomorphic prosthetic hands: a review. J Rehabil Res Dev 50(5):599–618
8. Shin YJ, Lee HJ, Kim K-S (2012) A robot finger design using a dual-mode twisting mechanism to achieve high-speed motion and large grasping force. T-RO 28(6):1398–1405
9. Jeong SH, Kim K-S, Kim S (2017) Designing anthropomorphic robot hand with active dual-mode twisted string actuation mechanism and tiny tension sensors. RA-L 2(3):1571–1578
10. Jeong SH, Kim K-S (2018) A 2-speed small transmission mechanism based on twisted string actuation and a dog clutch. RA-L 1571–1578
11. Kim S, Sim J, Park J (2020) Elastomeric continuously variable transmission combined with twisted string actuator. RA-L 5(4):5477–5484
12. O'Brien KW et al (2018) Elastomeric passive transmission for autonomous force-velocity adaptation applied to 3D-printed prosthetics. Sci Robot 3(23):1–9
13. Matsuchita K, Shikanai S, Yokoi H (2009) Development of drum CVT for a wire-driven robot hand. In: International conference on intelligent robots and systems (IROS), pp 2251–2256
14. Park J, Kim J-C, Nguyen CD, Kim K-S, Kim S (2018) A passively adaptive variable-radius pulley for a tendon-driven robotic joint. Mech Mach Theory 128:110–124
15. Takaki T, Omata T (2011) High-performance anthropomorphic robot hand with grasping-force-magnification mechanism. T-MECH 16(3):583–591
16. Liu H, Zhao B, Liu Z, Xu K (2020) Design of a lightweight single-actuator multi-grasp prosthetic hand with force magnification. J Mech Robot 12:1–10
17. Butin C, Chablat D, Aoustin Y, Gouaillier D (2022) Design of a two-speed load adaptive variable transmission for energetic optimization of an accessible prosthetic hand. J Mech Robot 15:1–11
18. Phlernjai M, Takayama T, Omatra T (2016) Passively switched cable-driven transmission for high-speed/high-force robot finger. Adv Robot 30(24):1559–1570
19. In H, Cho K-J (2013) Concept of variable transmission for tendon driven mechanism. In: International conference on ubiquitous robots and ambient intelligence (URAI), pp 15–16
20. Wilkie DR (1950) The relation between force and velocity in human muscle. J Physiol 110(3–4):249–280
21. Chen W, Xiong C, Chen W, Yuec S (2018) Mechanical adaptability analysis of underactuated mechanisms. Robot Comput Integr Manuf 49:436–447
22. Tilley AR, Associates HD (2001) The measure of man and woman: human factors in design, revised edition. Wiley, New York
23. Kong Y-K, Lowe BD (2005) Optimal cylindrical handle diameter for grip force tasks. Int J Ind Ergon 35(6):495–507
24. Vinet R, Lozac'h Y, Beaudry N, Drouin G (1995) Design methodology for a multifunctional hand prosthesis. J Rehabil Res Dev 32(4):316–324
25. Dechev N, Cleghorn W, Naumann S (2001) Multiple finger, passive adaptive grasp prosthetic hand. Mech Mach Theory 36(10):1157–1173